Available online at www.sciencedirect.com

ScienceDirect

The Journal of Finance and Data Science 8 (2022) 309–330

http://www.keaipublishing.com/en/journals/jfds/

Vine copula based dependence modeling in sustainable finance

Claudia Czado [a,b,*], Karoline Bax [c,f], Özge Sahin [a,b], Thomas Nagler [d,e], Aleksey Min [a], Sandra Paterlini [c]

[a] *Department of Mathematics, Technical University of Munich, Munich, Germany*
[b] *Munich Data Science Institute, Garching, Germany*
[c] *Department of Economics and Management, University of Trento, Trento, Italy*
[d] *Department of Statistics, Ludwig Maximilian University of Munich, Munich, Germany*
[e] *Munich Center for Machine Learning, Munich, Germany*
[f] *TUM School of Management, TUM Campus Heilbronn, Technical University of Munich, Heilbronn, Germany*

Received 24 October 2022; revised 11 November 2022; accepted 13 November 2022
Available online 17 November 2022

Abstract

Climate change and sustainability have become societal focal points in the last decade. Consequently, companies have been increasingly characterized by non-financial information, such as environmental, social, and governance (ESG) scores, based on which companies can be grouped into ESG classes. While many scholars have questioned the relationship between financial performance and risks of assets belonging to different ESG classes, the question about dependence among ESG classes is still open. Here, we focus on understanding the dependence structures of different ESG class indices and the market index through the lens of copula models. After a thorough introduction to vine copula models, we explain how cross-sectional and temporal dependencies can be captured by models based on vine copulas, more specifically, using ARMA-GARCH and stationary vine copula models. Using real-world ESG data over a long period with different economic states, we find that assets with medium ESG scores tend to show weaker dependence to the market, while assets with extremely high or low ESG scores tend to show stronger, non-Gaussian dependence.

2000 MSC: 0000; 1111

Keywords: Copulas; Vine copulas; Cross sectional and temporal dependence; ESG; Sustainability

Contents

* Corresponding author. Department of Mathematics, Technical University of Munich, Munich, Germany
E-mail addresses: cczado@ma.tum.de (C. Czado), karoline.bax@tum.de (K. Bax), ozge.sahin@tum.de (Ö. Sahin), mail@nagler.com (T. Nagler), min@tum.de (A. Min), sandra.paterlini@unitn.it (S. Paterlini).
Peer review under responsibility of China Science Publishing & Media Ltd.

https://doi.org/10.1016/j.jfds.2022.11.003

1. Introduction

Sustainability and climate change has gained importance for companies, investors, practitioners, and academics. Concurrently, non-financial information, including environmental, social, and governance (ESG) data, has been increasingly included in the investment decision making process[1] in general and for socially responsible funds[2] in particular. Following the 2020 Global Sustainable Investment Review, sustainable investment reached USD 35.3 trillion in five major markets at the beginning of 2020, and 35.9% of total assets under management are invested sustainably.[3]

ESG scores aim to measure the level of ESG performance of a company.[1] The scores are available from different rating institutions (e.g., Refinitiv by Thomson Reuters, Bloomberg, Sustainalytics), which use different quantitative and qualitative methods to assign an ESG score to a company. In brief, a high ESG score indicates ESG responsible behavior, while a low ESG score indicates ESG irresponsible behavior. Typically a company is associated with a rating class (e.g., *A*, *B*, *C*, or *D*) based on its ESG score. For example, within Refinitiv, assets are given a *D* grade for an ESG score lower than 25, *C* for an ESG score between 25 and 50, *B* for an ESG score between 50 and 75, and finally, *A* for an ESG score higher than 75.

As the economic and financial markets become more intertwined, and rapid advancements in technology and data processing are happening, academics and practitioners must find ways to model complex and interconnected systems. Traditional dependence measures often fail to create a complete understanding; therefore, copula models have been highlighted in the research community and gained popularity (e.g., Refs [4,5,6] for financial and risk applications).

A big advantage of copula models, proven by Sklar[7]; is that they can separately model marginal distributions and dependence structures of a given data. However, standard copula models cannot accommodate asymmetric tail dependence. Vine copula models were designed to increase the flexibility of these models. They rely on a pair copula construction and allow for modeling d-dimensional dependence structure by using two-dimensional building blocks and conditioning.[8,9] Standard vine copula models can assess only cross-sectional dependence. However, Nagler et al. (2022)[10] derived a stationary (S-) vine copula model that allows for simultaneously modeling cross-sectional and temporal dependencies. By showing that invariance is a sufficient condition for stationarity in this copula class, both types of dependencies can be modeled concurrently. The S-vine copula model includes a general vine structure for cross-sectional dependence and leaves flexibility for linking them across time.

While the ESG literature is dominated by various analyses on the relationship between ESG scores and financial performance or risk measures, the number of works combining vine copulas and ESG scores has increased too. These include but are not limited to Bax et al. (2021),[11] who used vine copulas to introduce new risk measures to assess if companies with similar ESG scores share similar risk characteristics. Further, Lööf et al (2022).[12] used copula-augmented predictive models and ESG-constrained optimization to assess the portfolio performance, focusing on

[1] The terms company and asset will be used interchangeably.

timber and forestry stocks. Also, Górka and Kuziak (2022) [13] included copulas to model volatilities and find diversification benefits. Others have focused on explaining how ESG scores are combined using a Random Forest algorithm.[14]

We focus on exploring complex dependencies between ESG indices and the market using different classes of vine copula models. More specifically, we use an ARMA-GARCH vine copula model as well as a S-vine copula model in our illustrations. This allows a first analysis of the inherent dependencies in ESG finance. Moreover, we guide how such models can be used in future research for this domain. In our analysis, we present that especially the extreme ESG classes (i.e., *A* and *D*) show strong cross-sectional dependencies with the US market, while the *B* class exhibit weaker dependence. Further, using dynamic vine copulas, we highlight that temporal dependence in the US market exists and is strongest in times of crisis and the most recent years.

The remainder is structured as follows. Section 2 gives a thorough introduction to dependence modeling with vine copulas. After discussing the ESG data set in Section 3, we build and interpret two different types of vine copula models for the dependence between ESG indices. In Section 4, we model temporal dependence for each index with ARMA-GARCH models and capture cross-sectional dependence between indices by a vine copula for the time series residuals. In Section 5, we explain and apply stationary vine copulas, which capture both types of dependence in a single model. Section 6 summarizes the paper and gives a future outlook.

2. Introduction to vine copula models

Copulas. The copula approach for constructing multivariate models is useful if we need to build a joint model with heterogeneous components such as for assets from different sectors and markets or from different ESG classes. Here arbitrary models for each component can be used. They are linked with a copula characterizing the dependence among the components. A d-dimensional *copula* C is a multivariate distribution function with values in $[0,1]^d$ with uniformly distributed margins. In the continuous case (which we assume from now on) the *copula density* can be obtained by partial differentiation. A fundamental representation of any distribution function in terms of a copula and its margins were proven in Ref [7]. In particular we have for a d-dimensional random vector $\boldsymbol{X}$ with joint and marginal distribution functions given by F and F_j, respectively and copula C

$$F(x_1, \ldots, x_d) = C(F_1(x_1), \ldots, F_d(x_d)). \tag{1}$$

This implies the multivariate density $f(x_1, \ldots, x_d) = c(F_1(x_1), \ldots, F_d(x_d))f_1(x_1)\cdots f_d(x_d)$, where f_j are marginal densities and c the copula density. By inversion of (1) we can use any d-dimensional distribution function to obtain the corresponding copula. Examples are the multivariate Gaussian and the Student t copula. Generator functions are used for the class of parametric Archimedean copulas, which includes the Gumbel, Clayton and Frank copula families. Two-parameter BB copula class allows for different, non-zero upper and lower tail behavior[15]; (Section 5.2).

To enhance the flexibility of bivariate copulas their survival and reflection versions can used. For example, the survival version of a bivariate copula density c is given by $c(u_1, u_2) = c(1 - u_1, 1 - u_2)$.

The case $d = 2$ plays a special role by being the building block for vine copulas. Further we need the conditional density $f_{1|2}$ and distribution function $F_{1|2}$ given by

$$f_{1|2}(x_1|x_2) = c_{12}(F_1(x_1), F_2(x_2))f_1(x_1) \tag{2}$$

$$F_{1|2}(x_1|x_2) = \frac{\partial}{\partial v} C_{12}(F_1(x_1), v)|_{v=F_2(x_2)}. \tag{3}$$

Dependence measures. Since copulas capture non linear dependence, the linear Pearson correlation dependence measure is inappropriate, instead Kendall's τ is often utilized. It is defined as

$$\tau(X_1, X_2) = P((X_{11} - X_{21})(X_{12} - X_{22}) > 0) - P((X_{11} - X_{21})(X_{12} - X_{22}) < 0),$$

where (X_{11}, X_{12}) and (X_{21}, X_{22}) are independent and identically distributed copies of (X_1, X_2). Kendall's τ is invariant with regard to marginal distributions and, therefore, depends only on the underlying copula. In finance we are interested in the dependence among extreme events and thus bivariate measures such as the tail dependence coefficients given by

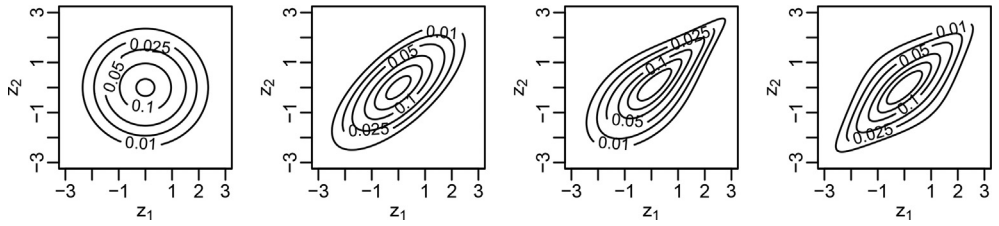

Fig. 1. Examples of marginally normalized contour plots. From left to right: Independence, Gaussian, Gumbel, Student t copulas.

$$\lambda^{upper} = \lim_{t\to 1^-} P\big(X_2 > F_2^{-1}(t) \big| X_1 > F_1^{-1}(t)\big) = \lim_{t\to 1^-} \frac{1-2t+C(t,t)}{1-t}$$

$$\lambda^{lower} = \lim_{t\to 0^+} P\big(X_2 \le F_2^{-1}(t) \big| X_1 \le F_1^{-1}(t)\big) = \lim_{t\to 0^+} \frac{C(t,t)}{t}.$$

are of interest. The Gaussian and Frank copulas do not exhibit tail dependence, while the Student t copula has symmetric tail dependence. The Clayton and Gumbel copula have only lower or upper tail dependence, respectively.

Visualizing copulas. Marginally normalized contour plots are used to compare bivariate copula families visually. For this we need the marginally normalized scale $(Z_1, Z_2) = \big(\Phi^{-1}\big(F_1(X_1)\big), \Phi^{-1}(F_1(X_2))$, where Φ denotes the $N(0, 1)$ distribution function. Since (Z_1, Z_2) has $N(0, 1)$ margins and so any non-elliptical contour indicates a deviation from Gaussian dependence. Fig. 1 shows normalized contour plots for some bivariate families. The circle in the leftmost panel corresponds to independence; the elliptical shape in the next panel to a Gaussian copula. Deviations from Gaussian dependence are visible in the two right panels. The first, a Gumbel copula, shows a spike in the upper-right tail indicating upper tail dependence. The rightmost panel is a Student t copula, which has symmetric tail-dependence in both tails.

Estimation. For parametric models with a small number of parameters in Equation (1) both the marginal and copula parameters can be estimated jointly by maximum likelihood. If this is not the case a two step approach is more tractable. In particular, we use independent and identically distributed (*i.i.d.*) observations $\boldsymbol{x}_i = (x_{i1}, \ldots, x_{id})$, $i = 1, \ldots, n$ to estimate the marginal parameters for the d marginal models separately yielding estimated marginal distribution functions $\widehat{F}_j, j = 1, \ldots, d$. They are used to create the *pseudo copula data*

$$\boldsymbol{u}_i = (u_{i1}, \ldots, u_{id}) = (\widehat{F}_1(x_{i1}), \ldots, \widehat{F}_d(x_{id})), \qquad i = 1, \ldots, n. \tag{4}$$

Copula parameter estimates are then based on the data from Equation (4). If parametric margins are used, the approach is known as inference for margins (IFM) approach,[16] while the semiparametric approach uses empirical margins.[17]

Pair copula decompositions. There are many choices for bivariate parametric copula families, but this is not true for $d > 2$. This raises the question: Can we utilize only bivariate copulas as building blocks to construct a d dimensional copula? In Ref. [18], conditioning was used for such a construction, and the first *pair copula construction* for distribution functions was given, while Bedford and Cooke (2002)[19] developed them for densities and provided a framework to identify all possible constructions. For the convenience of the reader, we show the basic ideas for $d = 3$ by utilizing the recursive factorization

$$f(x_1, x_2, x_3) = f_{3|12}(x_3|x_1, x_2) f_{2|1}(x_2|x_1) f_1(x_1) \tag{5}$$

and evaluate each term separately using $F_{j|D}$ and $f_{j|D}$ for the conditional distribution or density function of X_j given $\boldsymbol{X}_D$, respectively. For $f_{3|12}(x_3|x_1, x_2)$, we consider the bivariate conditional density $f_{13|2}(x_1, x_3|x_2)$. The copula density $c_{13;2}(\cdot, \cdot; x_2)$ denotes the copula density associated with the conditional distribution of (X_1, X_3) given $X_2 = x_2$. Using the density representation of (1) for $f_{13|2}(x_1, x_3|x_2)$ we have

$$f_{13|2}(x_1, x_3|x_2) = c_{13;2}(F_{1|2}(x_1|x_2), F_{3|2}(x_3|x_2); x_2) f_{1|2}(x_1|x_2) f_{3|2}(x_3|x_2). \tag{6}$$

The density of X_3 given $X_1 = x_1$, $X_2 = x_2$, denoted by $f_{3|12}(x_3|x_1, x_2)$, is determined from (2) applied to (6), yielding

$$f_{3|12}(x_3|x_1, x_2) = c_{13;2}(F_{1|2}(x_1|x_2), F_{3|2}(x_3|x_2); x_2) f_{3|2}(x_3|x_2). \tag{7}$$

Finally, direct application of (3) allows $f_{2|1}(x_2|x_1)$ and $f_{3|2}(x_3|x_2)$ to be expressed in terms of bivariate copulas. Using this together with (7) results in a *pair copula decomposition* of $f(x_1, x_2, x_3)$ as

$$\begin{aligned} f(x_1,x_2,x_3) = c_{13;2}\big(F_{1|2}(x_1|x_2), F_{3|2}(x_3|x_2); x_2\big) \times c_{23}(F_2(x_2), F_3(x_3)) \\ \times c_{12}(F_1(x_1), F_2(x_2)) f_3(x_3) f_2(x_2) f_1(x_1). \end{aligned} \tag{8}$$

Thus, the joint density can be expressed in terms of bivariate *pair copula* densities, marginal densities, and conditional distribution functions. It is not unique, since reordering the variables in (5) gives two further decompositions:

$$\begin{aligned} f(x_1,x_2,x_3) = c_{23;1}(F_{2|1}(x_2|x_1), F_{3|1}(x_3|x_1); x_1) \times c_{13}(F_1(x_1), F_3(x_3)) \\ \times c_{12}(F_1(x_1), F_2(x_2)) f_3(x_3) f_2(x_2) f_1(x_1) \end{aligned} \tag{9}$$

$$\begin{aligned} f(x_1,x_2,x_3) = c_{12;3}(F_{1|3}(x_1|x_3), F_{2|1}(x_2|x_1); x_3) \times c_{13}(F_1(x_1), F_3(x_3)) \\ \times c_{23}(F_2(x_2), F_3(x_3)) f_3(x_3) f_2(x_2) f_1(x_1) \end{aligned} \tag{10}$$

Pair copula constructions. All decompositions have a conditional copula term $c_{ij;k}(\cdot, \cdot; x_k)$. To facilitate estimation, we normally neglect the dependence on the specific conditioning value x_k. This is called the simplifying assumption.[20,21] Under this assumption we have the simplified pair copula construction with copula parameter vector $\boldsymbol{\theta} = (\boldsymbol{\theta}_{12}, \boldsymbol{\theta}_{23}, \boldsymbol{\theta}_{12;3})$

$$\begin{aligned} f(x_1,x_2,x_3;\boldsymbol{\theta}) = c_{13;2}\big(F_{1|2}(x_1|x_2), F_{3|2}(x_3|x_2); \boldsymbol{\theta}_{13;2}\big) \times c_{23}(F_2(x_2), F_3(x_3); \boldsymbol{\theta}_{23}) \\ \times c_{12}(F_1(x_1), F_2(x_2), \boldsymbol{\theta}_{12}) f_3(x_3) f_2(x_2) f_1(x_1). \end{aligned} \tag{11}$$

Here $c_{13;2}(\cdot, \cdot; \boldsymbol{\theta}_{13;2})$, $c_{12}(\cdot, \cdot; \boldsymbol{\theta}_{12})$ and $c_{23}(\cdot, \cdot; \boldsymbol{\theta}_{23})$ are arbitrary parametric bivariate copula densities. The dependence on marginal parameters has been suppressed to ease notation. This is no longer a decomposition but a construction, where the dependence on x_2 in $c_{13;2}(F_{1|2}(x_1|x_2), F_{3|2}(x_3|x_2); \boldsymbol{\theta}_{13;2})$ is solely captured by the arguments. If the margins in Equation (11) are uniform (*i.e.*, $f_j = 1$), we have a three-dimensional parametric copula density.

Parameter estimation. To estimate the parameter $\boldsymbol{\theta}$ using the i.i.d. sample $\boldsymbol{x}_i = (x_{i1}, x_{i2}, x_{i3})$, $i = 1, \ldots, n$ the two-step approach is followed. For this we construct the associated pseudo data $u_{i,j}$ as in (4) yielding the joint (pseudo-)likelihood for the copula density associated with (11) as

$$\begin{aligned} \ell(\boldsymbol{\theta}; \boldsymbol{u}) = \prod_{i=1}^{n} c_{13;2}\big(C_{1|2}(u_{i,1}|u_{i,2}; \boldsymbol{\theta}_{12}), C_{3|2}(u_{i,1}|u_{i,2}; \boldsymbol{\theta}_{23}); \boldsymbol{\theta}_{13;2}\big) \\ \times c_{23}(u_{i,2}, u_{i,3}; \boldsymbol{\theta}_{23}) \times c_{12}(u_{i,1}, u_{i,2}; \boldsymbol{\theta}_{12}). \end{aligned} \tag{12}$$

The joint maximum likelihood estimator $\widehat{\boldsymbol{\theta}}$ maximizes Equation (12). We describe now the alternative *sequential estimation method*, which remains computationally tractable in high dimensions. Maximizing over $\boldsymbol{\theta}_{12}$ and $\boldsymbol{\theta}_{23}$, respectively,

$$\prod_{i=1}^{n} c_{12}(u_{i,1}, u_{i,2}; \boldsymbol{\theta}_{12}) \quad \text{and} \quad \prod_{i=1}^{n} c_{23}(u_{i,2}, u_{i,3}; \boldsymbol{\theta}_{23})$$

to obtain $\widehat{\boldsymbol{\theta}}_{12}$ and $\widehat{\boldsymbol{\theta}}_{23}$. Then we create pseudo observations

$$u_{i,1|2,\widehat{\boldsymbol{\theta}}_{12}} = C_{1|2}(u_{i,1}|u_{i,2}; \widehat{\boldsymbol{\theta}}_{12}) \quad \text{and} \quad u_{i,3|2,\widehat{\boldsymbol{\theta}}_{23}} = C_{3|2}(u_{i,3}|u_{i,2}; \widehat{\boldsymbol{\theta}}_{23}), \tag{13}$$

for $i = 1, \ldots, n$. This is an approximate i.i.d sample from the pair copula $C_{13;2}$ under the simplifying assumption. Additionally, the marginal distribution of the pseudo observations (13) is approximately uniform, since (13) is a probability integral transform with estimated parameter values. Thus, we estimate the parameter(s) of the pair copula $c_{13;2}$ by maximizing

$$\prod_{i=1}^{n} c_{13;2}(u_{i,1|2,\widehat{\boldsymbol{\theta}}_{12}}, u_{i,3|2,\widehat{\boldsymbol{\theta}}_{23}}; \boldsymbol{\theta}_{13;2})$$

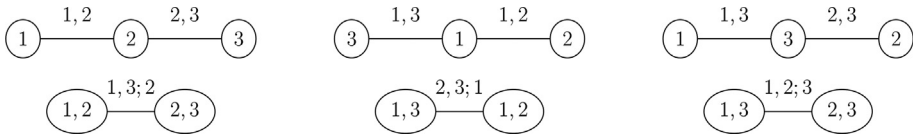

Fig. 2. Graphical representation of the pair copula constructions in three dimensions (left) $c_{12} - c_{23} - c_{13;2}$, (middle) $c_{13} - c_{12} - c_{23;1}$, and (right) $c_{13} - c_{23} - c_{12;3}$.

over $\boldsymbol{\theta}_{13;2}$, i.e. $\boldsymbol{\theta}$ can be estimated by solving three simpler problems. This estimate can also be used as a starting value for joint maximum likelihood estimation. A similar approach can also be followed when estimating pair copulas nonparametrically.[22,23]

Regular vine structures. In higher dimensions we need a graphical tool to identify different pair copula constructions. Such a tool was developed by Cooke and Bedford (2002)[9] and is called the *vine tree structure*. The corresponding tree structure consisting of two trees for the constructions (8)–(10) (from left to right) are shown in Fig. 2. The first tree identifies unconditional pairwise dependencies and the second tree conditional dependencies. More precisely, the nodes of the first tree indicate the variables X_1, X_2, and X_3, respectively. The edges correspond to unconditional pair copulas. For example, (8) has the pair copulas c_{12} and c_{23}, which are represented by the edges $1-2$ and $2-3$ in the left panel of Fig. 2 in Tree 1. For Tree 2 edges of Tree 1 are turned into nodes for Tree 2, i.e. the edges 1–2 and 2–3 in Tree 1 become nodes in Tree 2 which are connected by an edge representing the pair copula $c_{13;2}(\cdot, \cdot; x_2)$. Here the conditioning variable 2 is identified as the common element of the nodes 1, 2 and 2, 3 in Tree 2. From this we see that the product of all pair copulas associated with edges in the vine tree structure give the joint vine copula density. The two right panels of Fig. 2 represent (9) and (10), respectively.

Vine tree structures can also be defined in d dimensions consisting out of $d-1$ linked trees. The linking consists of turning edges in Tree $(j-1)$ into nodes of Tree j. The edges of Tree j have then to satisfy the *proximity condition*. This condition only allows edges in Tree j between two nodes a an b if the two nodes considered as edges in the Tree $(j-1)$ share a common node. The precise mathematical definition of these *R-vine tree structures* were developed by Bedford and Cooke (2002)[9] and illustrations are given Chapter 5 of Czado (2019).[24]

There are two subclasses of R-vine tree structures. A *canonical (C-) vine tree structure* consists of stars for all trees. So in every tree there is a single node, called the *root*, that is connecting all the others. A C-vine tree structure can be identified by the order of root nodes. We will later use such a structure in 5 dimensions (Fig. 4).

In a *drawable (D-) vine tree structure* all trees are paths. In a D-vine tree sequence, the proximity condition implies that the specification of Tree 1 determines all other trees. To characterize a D-vine structure, we therefore only need to specify the path in the first tree, called the order of a D-vine. The tree structure of a D-vine can be drawn in a way that resembles a grape vine giving its name.[19] For $d = 3$ the C-vine and D-vine tree structure coincide (see Fig. 2).

Regular vine copulas and distributions. The R-vine tree structure is the building plan of a regular (R-) vine distribution for the random vector $\boldsymbol{X} = (X_1, \ldots, X_d)$. This distribution is specified by three components: (1) a set of marginal distributions, (2) a specified R-vine tree sequence and (3) a set of specified pair copulas $c_{a,b;D}$ for each edge in the R-vine tree sequence. Here a and b are singletons and D is a set of indices from $\{1, \ldots, d\}$ without a and b. Each such pair copula $c_{a,b;D}$ represents the copula of the conditional distribution of X_a and X_b given $\boldsymbol{X}_D$. Under the simplifying assumption each conditional pair copula $c_{a,b;D}$ does not depend on the specific conditioning value of $\boldsymbol{X}_D = \boldsymbol{x}_D$. In Bedford and Cooke (2002)[9] , the existence of such distributions were shown and a representation of the joint density given. It involves only products of marginal densities and pair copulas $c_{a,b;D}$. For example, for C- and D-vine structures with (root) order 1, …, d, respectively,

$$
\begin{aligned}
f_{1,\ldots,d}(x_1, \ldots, x_d) &= \left[\prod_{j=1}^{d-1}\prod_{i=1}^{d-j} c_{j,j+i;1,\ldots,j-1}\right] \times \left[\prod_{k=1}^{d} f_k(x_k)\right], \\
f_{1,\ldots,d}(x_1, \ldots, x_d) &= \left[\prod_{j=1}^{d-1}\prod_{i=1}^{d-j} c_{i,(i+j);(i+1)\ldots,(i+j-1)}\right] \cdot \left[\prod_{k=1}^{d} f_k(x_k)\right].
\end{aligned}
$$

Here the index j identifies the tree level and the index i is used to enumerate the edges of that tree. The arguments of the copula terms were omitted in the last display. In general, these terms take the form $c_{a,b;D}(F_{a|D}(x_a|\boldsymbol{x}_D), F_{b|D}(x_b|\boldsymbol{x}_D))$. The conditional distribution functions in the arguments of $c_{a,b;D}$ can be determined recursively from conditional distributions of pair copulas occurring in earlier vine trees as shown in[15]. More details can be found in Chapter 5 of Czado (2019).[24]

Estimation and model selection. To apply vine copula models in practice, we have to perform three tasks of increasing complexity: (1) estimate parameters of a given pair copula model, (2) select an appropriate parametric family for a given pair copula, (3) decide on the tree structure determining which pair copulas are part of the model.

Task (1) is solved using the sequential estimation approach discussed earlier. Here we extend the construction of the pseudo data from tree T_2 given in (13) to trees T_3 to T_{d-1} using estimated conditional copula distribution functions. This is fast, since it allows to estimate the parameters of each pair copula term separately, starting from tree T_1 until T_{d-1}. The asymptotic properties of such parameter estimators, including standard errors are studied.[25,26]

For task (2), we also proceed sequentially and consider each pair copula separately. We fit the parameters for each family of the candidate list and choose the one which minimizes the Akaike Information Criterion (AIC)[27] or the Bayesian Information Criterion (BIC).[28]

Task (3) is the most challenging, since the number of vine tree structures grows superexponentially.[29] For $d = 10$ the number of regular vine tree structures is approximately 5×10^{14}. Even if we restrict to C- and D-vines, there are almost 2 million structures to be investigated. A greedy selection algorithm, called the Dissmann algorithm, has been developed in Ref.[30] It fits the strongest dependencies first. This is natural since estimation errors are propagated in the sequential estimation approach, and we may hope to find sparse models. To measure the strength of dependence, the empirical Kendall's τ is used. The Dissmann algorithm selects tree T_1 by using a maximal spanning tree algorithm with weights given by the absolute value of empirical Kendall's τ between any pair of variables. Once tree T_1 is determined, all pair copula families and parameters are selected and estimated using the approaches outlined for Tasks (1) and (2). For tree T_2, all possible edges allowed by the proximity condition are considered. On them, we find a spanning tree maximizing the absolute Kendall's τ computed from the pseudo data as defined in (13). We continue that way until all trees, pair copula families and its parameters are selected.

These methods are implemented very efficiently in C++ with interface to R in rvinecopulib,[31] which we will utilize for our data analyses. The computational demand typically scales quadratically with the dimension d, but the library has been applied for dimensions about $d = 400$. Other open source implementations in Matlab and Python are available.[32,33]

3. Data

In both illustrations in Sections 4 and 5.2, the data of ESG scores has been provided by Refinitiv, the risk business unit of Thomson Reuters. ESG scores are rank based, have values between zero and 100 and aim to measure the company's relative ESG performance, commitment, and effectiveness across ten main topics (e.g., emissions, resource use, and human rights).[34] Over time companies have improved their ESG scores as visible in Fig. 3 since they are under much pressure from the public and investors, and sustainability has become a core topic to deal with explicitly.

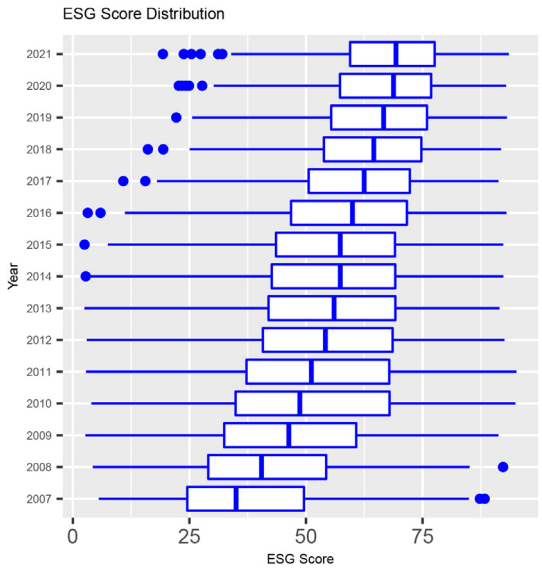

Fig. 3. Distribution of ESG scores of 330 assets of the S&P 500.

In our analyses, we consider the ESG class indices, which we compute using daily logarithmic returns and yearly ESG data of 330 US companies ($j = 1, \ldots, 330$), constituents of the S&P 500 index, from 4 January 2007 to 31 December 2021.[2] Additionally, we record the economic sector information of each asset and its market capitalization weights. Further we download the S&P 500 index for the same period to act as the market index ($I^q_{t,M}$) in our models from Thomson Reuters.

The chosen period (2007–2021) allows for having the largest number of assets and longest period to get a complete picture of crisis versus non-crisis times. We do so by splitting the overall period into five parts to compare different economic periods q: $q_1 = 2007$–2009, $q_2 = 2010$–2012, $q_3 = 2013$–2015, $q_4 = 2016$–2018 and $q_5 = 2019$–2021. Here q_1 captures the financial crisis period, and q_5 captures the beginning of the Covid-19 crisis. ESG scores in periods q_4 and q_5 are not definitive as they were not yet five years old when retrieving the data.[34] The data provider is, therefore, still able to modify these scores post-publication.

To compute the ESG class indices, we start by computing the mean ESG score ($E\,SG^q_j$) for each asset j in each period q. Then, since ESG scores are computed differently given the sector they belong to (see ref. [34]), we divide the assets into ten economic sectors. Within each sector, we rank the assets according to their mean ESG score ($E\,SG^q_j$) and group them into four different quartiles in each period q: assets with the highest $E\,SG^q_j$ are grouped in ESG class A, assets with the lowest $E\,SG^q_j$ in ESG class D, and the assets with the second to highest and second to lowest performance in ESG classes B and C, respectively, in each sector. We use quartiles to cluster the assets and not just the thresholds defined by Refinitiv since ESG scores tend to improve over time as seen in Fig. 3. Hence, otherwise, we would have only a small number or even zero assets in class D in the last years. This process also allows us to take care of any sectorial differences.

Now we compute the ESG class indices per ESG class k and period q ($I^q_{t,k}$) as a linearly weighted combination of the daily (t) asset returns in the same ESG class, using the assets' market capitalization weights. For instance, the ESG class index A in period q on trading day t is $I^q_{t,A}$. Since these steps are done individually for each period q, assets can change the ESG class between periods and do not necessarily have to stay within the same class.

The input data for the vine copula based models is always the daily ESG class indices, $I^q_{t,k}$, in each period q. However, due to the differences in modeling, the data processing is not identical. Therefore, we add a flowchart in Figure A.6 to make for an easier understanding and illustrate the process in each corresponding section.

4. Vine copula based modeling with ARMA-GARCH margins

Marginal modeling. While the estimation and selection approach detailed in Section 2 are suitable for multivariate i.i.d. data, a filtering step is needed for time series observations, as is the case for the ESG data. To apply vine copulas, we choose an appropriate time series model, such as an ARMA-GARCH model,[35] for each univariate time series. Such an application removes the temporal dependence in each series. Then, using the innovation distribution in the ARMA-GARCH model, we construct standardized residuals (see the right branch of Figure A.6). The standardized residuals of each series will be approximately i.i.d. After transforming them to the copula scale, they will form the input of a vine copula model. We call this approach the *ARMA-GARCH vine copula modeling approach*. A short review of ARMA-GARCH models is given in Appendix D.3.

To illustrate the ARMA-GARCH vine copula modeling approach, we use the ESG class and market indices $I^q_{t,k}$ described in Section 3 as input data. For this data, ARMA(1,1)-GARCH(1,1) models with skewed Student innovations (sssd) were sufficient to remove the serial dependence for each of the five components. The estimated parameters are given in Table D.13. Next standardized residuals are used to form the pseudo copula data.

Vine structure. We now select the vine tree structure for ESG data: Since we expect the market index (S&P 500) to influence the different ESG class indices, we choose a star structure in the first tree to model their dependence, inducing a C-vine tree structure. Now we only need to select the root nodes of the remaining trees. Since there is a natural order among the four different ESG classes, the root nodes obey that order, e.g., the conditional dependence of the ESG class A given the market is modeled in the second tree. Fig. 4 shows the imposed vine tree structure, where the ESG class and market indices $I^q_{t,k}$ are abbreviated by $k \in \{A, B, C, D, M\}$ for easier notation.

[2] Date of retrieval was 28 April 2022.

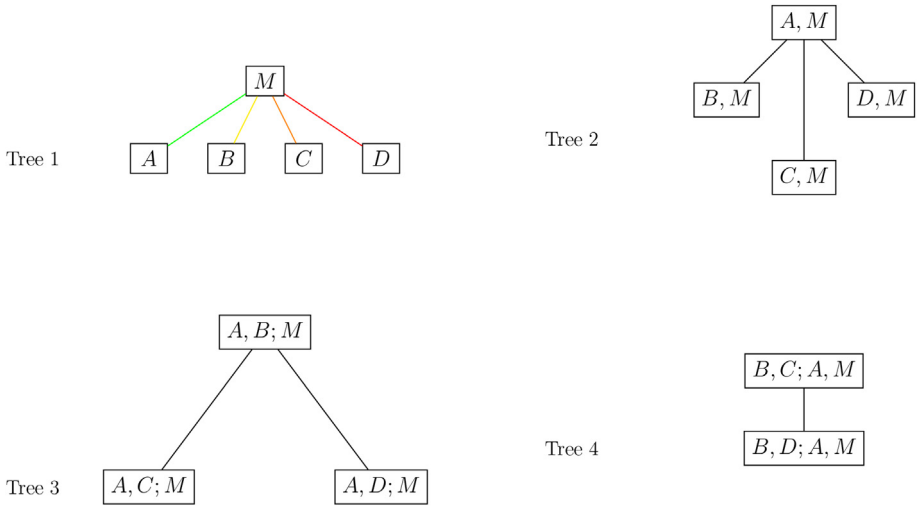

Fig. 4. Vine tree structure of the static vine copula model used in the dependence analysis of market and ESG class indices.

We can now study whether assets with different ESG classes show similar or different dependencies with the market index in various periods. In addition, the higher trees allow us to model other complex structures, such as the conditional dependence of the ESG classes C and D given others. The structure can, however, be adapted depending on which dependencies one is most interested in. Moreover, the vine structure can be chosen by the heuristic Dissmann algorithm as explained in Section 2. Thus, we also allow the vine tree structure to be chosen by this algorithm.

Estimation and model selection. We select the pair copula families and their parameters of the associated vine tree structure tree by tree, starting from Tree 1, as proposed in[30]. For the pair copula family selection, we allow all bivariate copula families implemented in[31] and choose the one with the lowest AIC. The pair copula family and its parameter(s) for each edge in the vine structure are selected and estimated as discussed in Section 2.

The results for the vine structures imposed and chosen by the heuristic Dissmann algorithm in terms of the AIC and BIC are given in Appendix D.2. We find that the imposed C-vine tree structure in Fig. 4 provides better model fits than the other in all periods but 2019–2021.

Interpretation. Results of the imposed C-vine tree structure (Fig. 4) for the first three trees are in Tables 1–3. We report the selected pair copula families, their estimated dependencies and the resulting lower and upper tail dependence coefficients. For easier understanding, we color the edges of the first tree of Fig. 4, whose results in Table 1 have the same color.

Table 1 shows that the market index has the strongest dependence on the ESG classes C and A during the crisis (2007–2009) and A and B during the Covid-19 period (2019–2021). ESG class D has the smallest dependence on the market index in these two crisis periods. During calm periods (2010–2012 and 2013–2015), we find the strongest dependence in the extreme ESG classes A and D. Moreover, in these calm periods, the market index and ESG class C show the lowest dependence compared to the other classes. In the most recent period, the ESG classes A and B and the market index M show the strongest dependence. A similar result is also visible for the lower and upper tail dependence coefficients. The lower and upper tail dependence coefficients between an ESG class and market indices are the highest for C and A during the crisis (2007–2009), while D exhibits the weakest dependence.

Some explanation of these results could be related to the size effect. Research has shown that larger companies are more likely to be awarded an ESG score[36] while other scholars have shown that companies with higher market capitalization tend to have higher ESG scores.[37] We would like to note that also, in our sample, the assets in class A tend to have the largest market capitalization compared to assets in other ESG classes.[3] These companies tend to have more capital and managerial support to push for sustainability changes and disclosure. Additionally, these companies tend to be more in the spotlight and feel societal pressure to make a positive change. Moreover, investors tend to flight to quality (i.e., class A); therefore, a lot of attention is given to ESG Class A during crisis periods, especially recent ones,

[3] Results are available upon request by the authors.

Table 1
ARMA-GARCH vine copula results ESG data for Tree 1 in different periods (rot = family's rotation, ltaildep/utaildep = lower/upper tail dependence coefficients).

Period	conditioned	family	rot	tau	ltaildep	utaildep
2007-2009	D, M	t	0	0.67	0.57	0.57
	C, M	BB7	0	0.82	0.93	0.87
	B, M	BB1	0	0.70	0.73	0.64
	A, M	BB7	0	0.81	0.92	0.87
2010-2012	D, M	BB7	180	0.80	0.88	0.89
	C, M	t	0	0.70	0.67	0.67
	B, M	BB7	0	0.74	0.84	0.80
	A, M	BB7	180	0.81	0.88	0.90
2013-2015	D, M	BB7	180	0.80	0.87	0.88
	C, M	t	0	0.70	0.65	0.65
	B, M	t	0	0.71	0.68	0.68
	A, M	BB7	180	0.79	0.87	0.87
2016-2018	D, M	BB1	0	0.77	0.78	0.74
	C, M	t	0	0.67	0.62	0.62
	B, M	BB1	180	0.76	0.74	0.75
	A, M	BB7	180	0.72	0.88	0.00
2019-2021	D, M	t	0	0.65	0.39	0.39
	C, M	BB7	0	0.73	0.84	0.79
	B, M	BB7	180	0.80	0.88	0.88
	A, M	BB7	180	0.80	0.88	0.87

Table 2
ARMA-GARCH vine copula results ESG data for Tree 2 in different periods (rot = family's rotation, ltaildep/utaildep = lower/upper tail dependence coefficients).

Period	conditioned	conditioning	family	rot	tau	ltaildep	utaildep
2007–2009	D, A	M	BB8	180	0.124	0	0
	C, A	M	t	0	0.003	0.046	0.046
	B, A	M	Frank	0	0.084	0	0
2010–2012	D, A	M	t	0	−0.057	0.017	0.017
	C, A	M	Frank	0	−0.171	0	0
	B, A	M	t	0	−0.216	0	0
2013–2015	D, A	M	t	0	−0.056	0.008	0.007
	C, A	M	t	0	−0.065	0.001	0.001
	B, A	M	Frank	0	−0.133	0	0
2016–2018	D, A	M	Joe	0	0.025	0	0.058
	C, A	M	Gumbel	90	−0.061	0	0
	B, A	M	Indep.	0	0	0	0
2019–2021	D, A	M	BB1	180	0.065	0.087	0
	C, A	M	t	0	0.123	0.036	0.036
	B, A	M	t	0	−0.078	0.016	0.016

Table 3
ARMA-GARCH vine copula results ESG data for Tree 3 in different periods (rot = family's rotation, ltaildep/utaildep = lower/upper tail dependence coefficients).

Period	conditioned	conditioning	family	rot	tau	ltaildep	utaildep
2007–2009	D, B	A, M	t	0	0.258	0.116	0.116
	C, B	A, M	Clayton	0	0.044	0.001	0
2010–2012	D, B	A, M	t	0	−0.130	0.001	0.001
	C, B	A, M	BB8	180	0.080	0	0
2013–2015	D, B	A, M	Gumbel	90	−0.147	0	0
	C, B	A, M	BB7	90	−0.098	0	0
2016–2018	D, B	A, M	t	0	−0.252	0	0
	C, B	A, M	Joe	180	0.054	0.120	0
2019–2021	D, B	A, M	t	0	−0.113	0	0
	C, B	A, M	Gumbel	90	−0.116	0	0

while such behavior is not needed in calmer periods. Thus, the size effect can offer some explanation to the results; however, as we use only a subset of the constituents of the S&P 500, there must also be additional factors involved that we cannot fully comprehend yet.

In Tree 2, ESG classes *A* and *D* conditioned on the market *M* show the strongest absolute dependence in crisis period 2007–2009 (Table 2). In the following two calm periods, the strongest absolute dependence is between ESG classes *A* and *B* conditioned on the market *M*. Even though the strongest absolute dependence is between the ESG classes *A* and *C* conditioned on the market *M* in the most recent period, such dependencies are lower than the strongest absolute dependence of the other periods. Moreover, the negative dependence of ESG classes *A* and *B* conditioned on the market *M* in 2010–2012 and 2013–2015 might imply that investors change their investment preferences among assets in high ESG classes during the calm periods.

In Tree 3 (Table 3), the strongest absolute dependence over all periods is between ESG classes *B* and *D* conditioned on the market *M* and *A* in 2007–2009. The large absolute dependencies of the ESG classes *A* and *D* (and, to an extent, *C*) can be explained by looking at investor behavior and preferences. As companies are under pressure to improve their ESG performance, investors increasingly focus on assets with a high ESG performance.[1] These assets, therefore, receive much attention. While assets in the lower ESG class experience the opposite effect by often being excluded from investment portfolios,[1] assets that are neither good nor bad in their ESG performance often do not play an important role in investment choices. By showing that these assets have low dependence on the market (Table 1), they could be used in hedging and mitigating market risk.

While we find some symmetric tail dependence (Student *t* copula) in each period, mostly BB7 and BB1 copulas with asymmetric tail dependence were fitted in the first tree in Table 1. In Table 2, we find that the dependence between class *B*, class *C*, class *D* and class *A* conditioned on the market is also non-Gaussian. Likewise, the dependence between class *B* and class *C*, as well as class *B* and class *D* conditioned on class *A* and market, is non-Gaussian as seen in Table 3. Such results show that a multivariate Gaussian distribution to model such dependencies cannot be adequate.

The results from Tree 4 are added to Appendix C for completeness.

5. Stationary vine copula based modeling

5.1. Stationary (S-) vines

The approach from the previous section separates modeling of dependence within a single time series from modeling the dependence across series. We can also build a single vine copula model for both types of dependence. In 2015, three such models were independently proposed by Beare and Seo (2015),[38] Brechmann and Czado (2015),[39] and Smith (2015),[40] and later generalized to the class of *stationary vines* or *S-vines* by Nagler et al. (2022).[10]

Suppose we observe a multivariate time series $\boldsymbol{X}_t = (X_{t,1}, \ldots, X_{t,d})$, $t = 1, \ldots, T$. The general idea is to build one large vine copula over all variables $j = 1, \ldots, d$ observed at all time points $t = 1, \ldots, T$. In such a model, each variable is identified by a tuple (t, j), where t is the time index and j the variable index. Naively, such a model requires the

specification of $T \times d$ marginal distributions, a $T \times d$-dimensional vine structure, and $Td(Td-1)/2$ pair-copulas, which is an intractable problem. However, time series usually have more structure, which might lead to simplifications. In particular, one normally assumes the time series to be *stationary*, i.e., the distribution of the variables is invariant to shifts in time. This imposes restrictions on both the marginal distributions and the pair-copulas. First, the marginal distributions $F_{t,j}$ of the variables $X_{t,j}$ has to be independent of the time index t. Hence, we only have to specify d marginal distributions F_j, $j = 1, \ldots d$. Similarly, the (conditional) dependence between variables has to be invariant to shifts in time. For example, the dependence between variables $X_{t,j}$ and $X_{t+1,k}$ conditional on $X_{t+1,j}$ must be the same as the dependence between $X_{t+\delta,j}$ and $X_{t+1+\delta,k}$ conditional on $X_{t+1+\delta,j}$ for any δ. Hence, the corresponding pair-copulas have to be identical as well. This restriction is called *translation invariance* of the pair-copulas.[38,10]

It was shown in Ref. [10] that stationarity of dependence is difficult to enforce for general vine structures. The reason is that only some of the (conditional) dependencies are explicit in the model (i.e., given by a specific pair-copula). However, they derived the maximal class of vine structures where translation invariance of the pair-copulas is sufficient to ensure stationarity of the full dependence structure. This is the class of *S-vine* structures. S-vines follow an intuitive building plan. First, we build a full vine structure $\mathcal{V}^{(0)}$ for the variables $(X_{1,1}, \ldots, X_{1,d})$, which we call the *cross-sectional vine*. This structure is copied to all time lags $(X_{t,1}, \ldots, X_{t,d})$, $t = 2, \ldots, T$. Next, we build a full vine structure for the variables $(X_{1,1}, \ldots, X_{1,d}, X_{2,1}, \ldots, X_{2,d})$ that contains the two copies of $\mathcal{V}^{(0)}$ and additional edges linking them. The additional d^2 edges have to be chosen in such a way that a valid vine tree structure for the $2d$ variables are obtained. Then this structure is copied across all lags, etc. More technical definitions and formal results can be found in Ref [10]. An example of such a structure with cross-sectional C-vines is shown in Fig. 5 and will be discussed in more detail shortly.

We can simplify the model further by assuming that the multivariate time series is a Markov chain. The series $(\boldsymbol{X}_t)_{t=1,\ldots,T}$ is called *p-Markovian* if the last p time points are sufficient for prediction, i.e.,

$$P(\boldsymbol{X}_t \leq \boldsymbol{x} | \boldsymbol{X}_{t-1}, \ldots, \boldsymbol{X}_1) = P(\boldsymbol{X}_t \leq \boldsymbol{x} \big| \boldsymbol{X}_{t-1}, \ldots, \boldsymbol{X}_{t-p}) \quad \text{for all } \boldsymbol{x} \in \mathbb{R}^d.$$

Theoretically, this condition implies a large number of independence copulas in higher trees of the S-vine model (see Ref [10] for more details). Practically, this means that we only need to build models for $p + 1$ consecutive time points (instead of all T time points).

The stationary D-vine and M-vine models of Beare and Seo (2015)[38] and Smith (2015)[40] are two special cases of S-vines, where the cross-sectional structure $\mathcal{V}^{(0)}$ is a D-vine. They differ only in how the cross-sectional parts are linked across time points. The COPAR model of Brechmann and Czado (2013)[39] follows a similar idea with cross-sectional C-vines, but links the cross-sectional trees in a way that does not ensure stationarity for an arbitrary choice of the set of translation invariant pair-copulas.

5.2. Illustration of stationary vine copula modeling in sustainable finance

We now illustrate how to build, fit, and interpret S-vine copula models on the ESG data of Section 3 using the `svines` R-package by.[41] This package is also based on the `rvinecopulib` library[31] and similarly efficient.

Marginal modeling. As usual, the first step is to find appropriate marginal models. Compared to the ARMA-GARCH vine models from Section 4, this is a lot easier, since we do not have to account for serial dependence. We merely have to find marginal distributions F_k for the ESG class and market indices $I^q_{t,k}$, $k \in \{A, B, C, D, M\}$. By the assumption of stationarity these distributions are invariant with respect to the time index t. For each index and period, we shall assume a parametric model $F^q_k(\cdot; \boldsymbol{\eta}^q_k)$, where $\boldsymbol{\eta}^q_k$ is the parameter vector for the k-th margin and q-th period. The parameters can be estimated by maximum-likelihood-type estimators

$$\widehat{\boldsymbol{\eta}}^q_k = \arg\max_{\boldsymbol{\eta}} \sum_{t \in \mathcal{T}_q} \ln f_k(I^q_{t,k}; \boldsymbol{\eta}),$$

where the summation index runs over all time points $\mathcal{T}_q$ in period q and f^q_k is the associated density to F^q_k. The estimated model for index k and period q is then $\widehat{F}^q_k = F^q_k(\cdot; \widehat{\boldsymbol{\eta}}^q_k)$. To find appropriate parametric models, we select from a set of suitable parametric families. Financial time series are known to exhibit heavy tails, so (skew) logistic, Student t or generalized error distributions may qualify. For each index and period, we choose the one that minimizes the AIC criterion. The marginal distributions and parameters used for the ESG data are given in Appendix B.

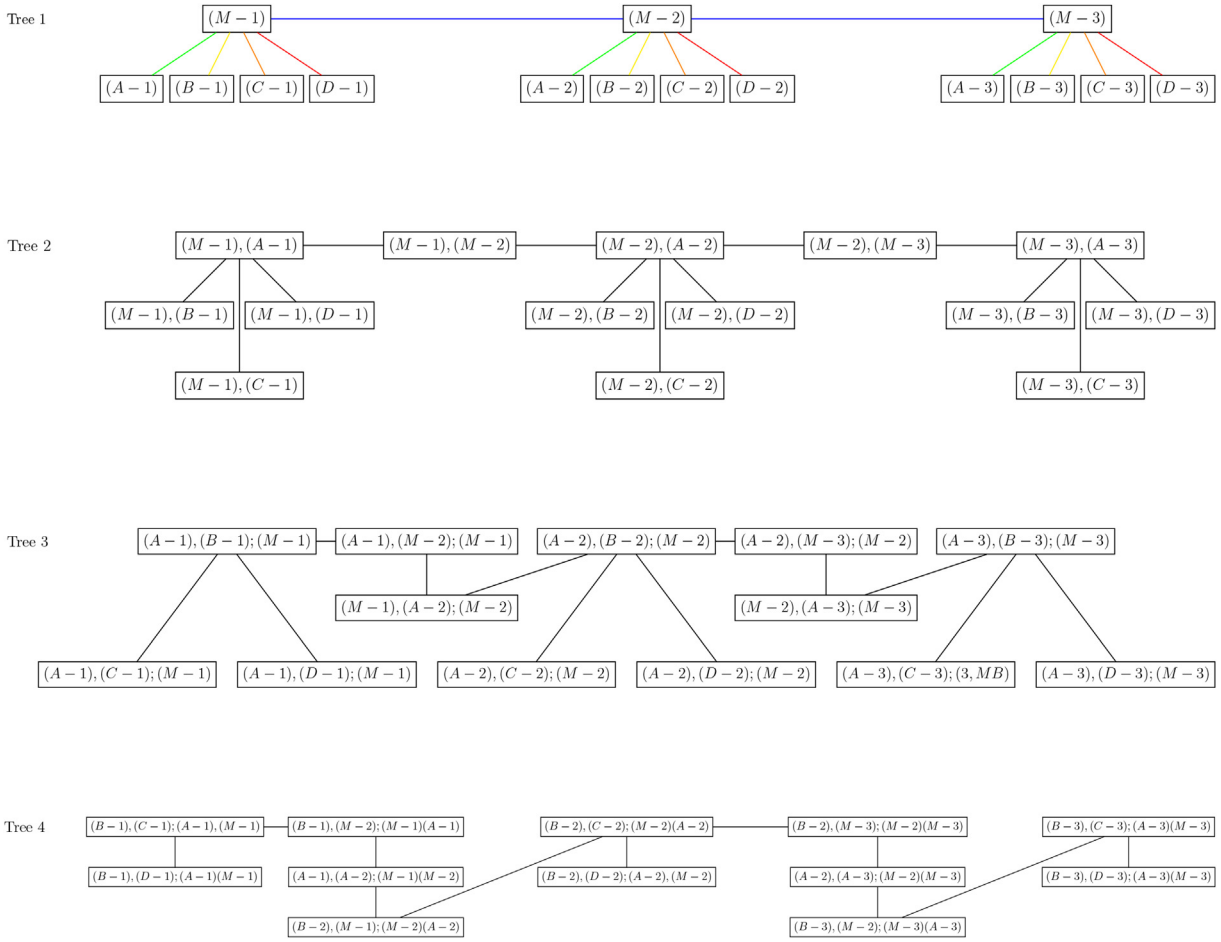

Fig. 5. Vine tree structure (the first four trees) of the dynamic vine copula used in the dependence analysis of market and ESG class indices on three time points (days).

As an alternative, one could also employ a nonparametric approach and model the margins by the empirical distribution function

$$\widehat{F}_k^q(x) = \frac{1}{|\mathcal{T}_q| + 1} \sum_t \mathbb{1}(I_{t,k}^q \leq x),$$

where the summation index t runs over all T_q time points in period q. This approach prevents misspecification of the parametric model, but cannot reproduce the heavy tails observed in financial time series well.

From the estimated marginal distribution functions $\widehat{F}_k^q$, we now generate pseudo-observations for the copula using $U_{t,k}^q = \widehat{F}_k^q(I_{t,k}^q), t \in \mathcal{T}_q$.

The S-vine structure. We move on to modeling the dependence. As explained in Section 5.1, S-vines follow a specific building plan. In particular, we have to specify the cross-sectional structure and the links across time points. Fig. 5 shows the first four trees of an S-vine structure for the indices $\{M, A, B, C, D\}$ observed at three points in time. For example, the node $M - 2$ corresponds to the market index at time $t = 2$. If we focus on only a single time point, we see a star-shaped graph corresponding to the cross-sectional C-vine. Copies of this C-vine appear on all three time points. It was shown in Ref. [10] that the links across time points are fully characterized by two permutations $\boldsymbol{\pi}^{\text{out}}$ and $\boldsymbol{\pi}^{\text{in}}$ of the indices $\{A, B, C, D, M\}$. The first entry in the permutations is the index, where two adjacent time points are linked in the

first tree level of the vine. In Fig. 5, the connecting edge goes from node $M-1$ at the first time point (so $\pi_1^{\text{out}} = M$) to node $M-2$ at the second (so $\pi_1^{\text{in}} = M$). This edge correspond to a node $(M-1, M-2)$ in the second tree of the structure. The second entries of the permutation indicate which variables are connected to this edge. There is an edge going from node $(A-1, M-1)$ into $(M-1, M-2)$ (so $\pi_2^{\text{out}} = A$) and another edge from $(M-1, M-2)$ to $(M-2, A-2)$ (so $\pi_2^{\text{in}} = A$). The full permutations are $\boldsymbol{\pi}^{\text{out}} = \boldsymbol{\pi}^{\text{in}} = (M, A, B, C, D)$. In general, the two permutations do not have to coincide and other permutations than the one in our example are possible. However, the permutations have to comply with the proximity condition mentioned in Section 2; a formal condition for compatibility is given in Ref. [10].

The S-vine structure in Fig. 5 is a natural extension of the C-vine structure we identified as suitable for the ESG data in Section 4. In particular, the C-vine from Section 4 is exactly the cross-sectional structure of the S-vine. Therefore, we further decided to link the trees in an order that corresponds to the importance of the indices, where we assume the market to be the main driver of dependence, followed by the ESG indices of decreasing quality.

Alternatively, one may also choose the S-vine structure in a data-driven manner. Similar to Dissman's heuristic, we then select the cross-sectional structure and connecting edges by building maximum-spanning trees according to dependence measures like Kendall's τ. The structure does influence not only model fit but also its interpretation; only the explicit dependencies corresponding to edges in the structure can be interpreted easily. If a certain structure is intuitive for the data, it is thus sometimes preferable to a data-driven choice. In the example of our ESG data, the custom structure in Fig. 5 also seems to provide a better fit (see Table D.12).

Estimation and model selection. The parameters of an S-vine copula model can be estimated in a tree-wise manner, similar to Section 2. The only difference is that many pair-copulas in the model are identical because of stationarity, so they only have to be estimated once. Further, the pair-copula families can be selected tree-wise according to the AIC or BIC criteria. Estimated pair-copulas for the first two trees on the ESG data are given in Tables 4 and 7. S-vine models pose the additional problem of choosing an appropriate Markov order p. A straightforward approach is to fit models for a few orders and select the order with the smallest AIC/BIC. For time series of financial returns, $p = 1$ or $p = 2$ is normally sufficient. Results for the ESG data are provided in Table D.12 and indicate that $p = 2$ is preferred in most periods.

Interpretation. Let us now discuss the estimated model and draw some comparisons to the ARMA-GARCH vine copula model from Section 4. The interpretation of cross-sectional pair-copulas in Tables 4 and 5 is rather straightforward: they describe the dependence between a (conditional) pair of indices, all observed at the same point in time. There is an important difference to the ARMA-GARCH vine model, where the pair-copulas describe the dependence between *residuals* of the marginal ARMA-GARCH models for each index. The dependencies in the S-vine model therefore have a more direct interpretation. Nevertheless, we notice that the values in Table 4 are very similar to those of the static vine copula model in Table 1. Thus, it turns out that the ARMA-GARCH effects are very small in our time series (see Appendix D.3).

Again, for the crisis period 2007–2009, we find that ESG classes A and C show the strongest dependence; afterward, it shifts to ESG classes A and D for the next three periods in the first tree in Table 4. Furthermore, the selected pair-copula families all feature both lower and upper tail dependence, often with slightly stronger lower than upper tail dependence. The cross-sectional pair-copulas of the second tree (Table 5) describe the dependence of two ESG indices conditional on the market (read: after the influence of the market has been accounted for). The dependencies are all quite weak. Though not yet negligible, this confirms our intuition that the market index drives much of the dependence among the ESG indices. This simple interpretation is facilitated by the structure in Fig. 5. Other cross-sectional structures would also feature conditional dependencies between the market and an ESG index conditional on another ESG index, for example, the dependence between class A and the market M given class C. Such dependencies are likely stronger and generally more difficult to interpret. The dependence between ESG classes A and B conditioned on the market M is stronger than the others in the first two calm periods in Table 5. For the crisis period 2007–2009, the strongest dependence is between ESG classes A and D conditioned on market M in the second tree. One possible interpretation is that in times of crisis, investors might put more attention to the highest ESG class A, hoping they would be more resilient or to the worst class D, considering them as the first investment option to discard. We omit results on dependencies in higher trees because they are weaker and more difficult to interpret.

Tables 6 and 7 show those pair-copulas from the first two tree levels that describe dependence across time points. In the first tree (Table 6), there is only one edge connecting subsequent time points, namely the one connecting the market index at time t and $t+1$. In most periods, a Student t copula with weak negative dependence and a small degree of

Table 4
Dependence across indices for each period q for Tree 1. These values and families are the same for $A-2, M-2$ and $A-3, M-3$ etc. as the tree structure is the same. (rot = family's rotation, ltaildep/utaildep = lower/upper tail dependence coefficients).

Period	conditioned	family	rot	tau	ltaildep	utaildep
2007-2009	D-1, M-1	t	0	0.69	0.69	0.69
	C-1, M-1	BB1	0	0.86	0.90	0.82
	B-1, M-1	BB7	180	0.73	0.82	0.81
	A-1, M-1	BB1	0	0.86	0.88	0.83
2010-2012	D-1, M-1	BB7	180	0.81	0.88	0.89
	B-1, M-1	BB7	180	0.69	0.79	0.74
	C-1, M-1	BB7	0	0.75	0.85	0.81
	A-1, M-1	BB7	180	0.81	0.88	0.91
2013-2015	D-1, M-1	BB7	180	0.79	0.87	0.88
	C-1, M-1	t	0	0.70	0.65	0.65
	B-1, M-1	t	0	0.70	0.68	0.68
	A-1, M-1	BB7	180	0.78	0.86	0.84
2016-2018	D-1, M-1	BB7	180	0.76	0.84	0.84
	C-1, M-1	t	0	0.69	0.66	0.66
	B-1, M-1	BB7	0	0.75	0.84	0.83
	A-1, M-1	BB7	0	0.82	0.91	0.88
2019-2021	D-1, M-1	BB7	0	0.70	0.81	0.77
	C-1, M-1	BB7	0	0.76	0.87	0.83
	B-1, M-1	BB7	180	0.81	0.88	0.90
	A-1, M-1	BB7	0	0.83	0.94	0.87

Table 5
Dependence across indices for each period q for tree 2. These values and families are the same for $D-2, A-2; M-2$ and $D-3, A-3; M-3$ etc. as the tree structure is the same. (rot = family's rotation, ltaildep/utaildep = lower/upper tail dependence coefficients).

Period q	conditioned	conditioning	family	rot	tau	ltaildep	utaildep
2007–2009	D-1, A-1	M-1	t	0	0.1397	0.042	0.042
	C-1, A-1	M-1	t	0	−0.0028	0.011	0.011
	B-1, A-1	M-1	t	0	0.0847	0.008	0.008
2010–2012	D-1, A-1	M-1	t	0	−0.0534	0.018	0.018
	C-1, A-1	M-1	BB8	270	−0.1778	0	0
	B-1, A-1	M-1	t	0	−0.220	0	0
2013–2015	D-1, A-1	M-1	t	0	−0.0578	0.009	0.009
	C-1, A-1	M-1	t	0	−0.0793	0.002	0.002
	B-1, A-1	M-1	Frank	0	−0.137	0	0
2016–2018	D-1, A-1	M-1	Indep.	0	0	0	0
	C-1, A-1	M-1	BB7	90	−0.0955	0	0
	B-1, A-1	M-1	t	0	−0.0334	0	0
2019–2021	D-1, A-1	M-1	BB8	90	−0.0410	0	0
	C-1, A-1	M-1	BB8	90	−0.1064	0	0
	B-1, A-1	M-1	BB8	270	−0.1598	0	0

Table 6
Dependence across indices for each period q for tree 1. These values and families are the same for $M-2, M-3$ as the tree structure is the same. (rot = family's rotation, ltaildep/utaildep = lower/upper tail dependence coefficients).

Period q	conditioned	family	rot	tau	ltaildep	utaildep
2007–2009	M−2, M-1	t	0	−0.078	0.044	0.044
2010–2012	M−2, M-1	Joe	270	−0.040	0	0
2013–2015	M−2, M-1	t	0	−0.046	0.048	0.048
2016–2018	M−2, M-1	t	0	−0.044	0.106	0.106
2019–2021	M−2, M-1	t	0	−0.076	0.137	0.137

Table 7
Dependence across indices for each period q for tree 2. These values and families are the same for $A-3, M-2; M-3$ and $A-2, M-1; M-2$ as the tree structure is the same. (rot = family's rotation, ltaildep/utaildep = lower/upper tail dependence coefficients).

Period q	conditioned	conditioning	family	rot	tau	ltaildep	utaildep
2007–2009	A-2, M-1	M-2	t	0	−0.035	0.023	0.023
	M−2, A-1	M-1	t	0	0.054	0.018	0.018
2010–2012	A-2, M-1	M-2	Indep.	0	0	0	0
	M−2, A-1	M-1	Indep.	0	0	0	0
2013–2015	A-2, M-1	M-2	BB8	180	0.045	0	0
	M−2, A-1	M-1	Indep.	0	0	0	0
2016–2018	A-2, M-1	M-2	Joe	90	−0.036	0	0
	M−2, A-1	M-1	Indep.	0	0	0	0
2016–2018	A-2, M-1	M-2	BB8	270	−0.048	0	0
	M−2, A-1	M-1	Indep.	0	0	0	0

freedom parameter was selected. Such a copula induces volatility clustering, which is typical in financial time series.[42] In the second tree (Table 7), there are two connecting edges. Both describe conditional dependence between the ESG class A index and the market index observed at different days. The first indicates how the market at time t depends with index A at time $t+1$, conditional on the market at time $t+1$. The second indicates how the market at time $t+1$ depends with index A at time t conditional on the market at time t. These pair-copulas serve two purposes at the same time. First, they induce the serial dependence for the ESG class A index, but in an indirect way (conditional on the market). This dependence is, therefore, rather difficult to interpret, which can be seen as a disadvantage compared to ARMA-GARCH vine models. The second purpose, however, is to model the cross-serial dependence between the market and index A at different time points, which can not be modeled explicitly in the former models. Overall, the results in Table 7 are rather incoherent across periods. Notably, only during the financial crisis 2007–2009, we observe tail dependence.

6. Summary and outlook

Sustainable finance aims at explicitly considering environmental, social and governance (ESG) factors when dealing with investments and companies. ESG scores and classes (A, B, C, and D) have become relevant information to take into account when making investment decisions and developing risk management and monitoring tools. Therefore, understanding the complex dependence relationships among ESG class indexes and the market index is of utmost importance, and vine copulas are possibly among the most appropriate tools to capture such dependencies.

While ARMA-GARCH vine copulas allow for modeling cross-sectional dependence after temporal dependence has been removed, stationary vine copulas allow for modeling both simultaneously. Based on the data provided by Refinitiv for the S&P500 Index and constituents, we show that the stationary vine copula models often fit better than the others concerning the AIC (Table D.12). Further, when modeling complex dependencies, the S-vine copulas allow for pointing out both the dependence across time and indices, providing a complete picture. However, their complex structure might make the interpretation harder than the ARMA-GARCH vine copula models.

Overall we find in times of crisis that assets in ESG class *A* and market *M*, as well as in ESG class *C* and market *M* show the strongest dependence. However, in calm periods, this relationship partially changes, and the strongest dependence is found between ESG class *A* and market *M*, as well as between ESG class *D* and market *M*. Assets not in the extreme ESG classes, which are neither very good nor bad, tend to show weaker dependence and could be considered for hedging or risk mitigation strategies regarding the market. An explanation for the high dependence in the extreme ESG classes could be investor preferences and attention to the most and least sustainable assets. In fact, exclusionary screening and best-in-class are typical investment strategies widely used, ending up putting more attention to the extreme classes during calm periods. During the crisis, ESG class *D* tends to be more weakly dependent, while ESG class *A* still exhibits high dependence. As the investment world is trying to get more sustainable, it is expected to observe such a level of pressure on assets in ESG class *A* as potentially due to the size effect and considered a flight to quality, while it is interesting to note that ESG class *D* might result in a weaker dependence.

Even though we focus on the dependence analyses of the ESG class indices and market index in the United States using a single data provider, we list some future research directions in sustainable finance using vine and stationary copulas as follows.

ESG risk dependence measures. From an investor's point of view, it is important to manage ESG-related risks in a portfolio. Thus, further analysis could focus on single assets to determine what part of ESG risk could be attributed to dependencies among assets belonging to the same ESG class, as suggested by.[11] This could also disentangle ESG risk dependence from the market and idiosyncratic risk. Naturally, as the model complexity increases, the model interpretability might suffer, but a more realistic picture of dependencies could allow for the development of more appropriate risk management and monitoring tools. Besides market risk, further applications might involve credit[43] or systemic risk.[44,45]

ESG data quality and measurement issues. Lately, there has been a hot debate about whether ESG scores are trustful measurements of companies' sustainable performance[46] and agreed upon by different data providers.[47] The way ESG scores are calculated and their impact on the financial performance or risk vary depending on the sector, topic, provider, and country.[48,49,50] Another important research study could analyze the dependence structure of the assets' ESG disclosure quality on various topics. It would highlight what seems important to disclose in ESG-related topics for companies.

Sustainable portfolio optimization. Optimal portfolio selection requires modeling dependence to promote diversification. Recently, numerous scholars, e.g., Pedersen et al. (2021)[51]; have proposed incorporating the ESG dimension into the portfolio selection problem. Copulas are a natural way of capturing such dependence, and one can expect large applications soon. In a similar context, for example,[52] compare the performance of ESG-based and conventional funds using vine copulas.

Finally, we like to add some general remarks on vine based modeling. Vines have found many applications in finance. For example, vines can be used to model market, credit, operational risk, and in portfolio optimization. The reader is referred to Ref. [53] and Chapter 11 of Ref. [24] and references therein for applications.

Further, vine copula based models can be used in a rolling window setup instead of the fixed time period approach followed here. This is very computationally costly and for the ARMA-GARCH vines this has been implemented in the R-package portvine of Ref. [54] to study forecasts of (conditional) risk measures in portfolios.

Funding

Claudia Czado is supported by the German Research Foundation (DFG grant CZ 86/6-1).

Conflicts of Interest

All authors have none to declare.

Appendix A. Data processing of ARMA-GARCH and stationary vine copula models

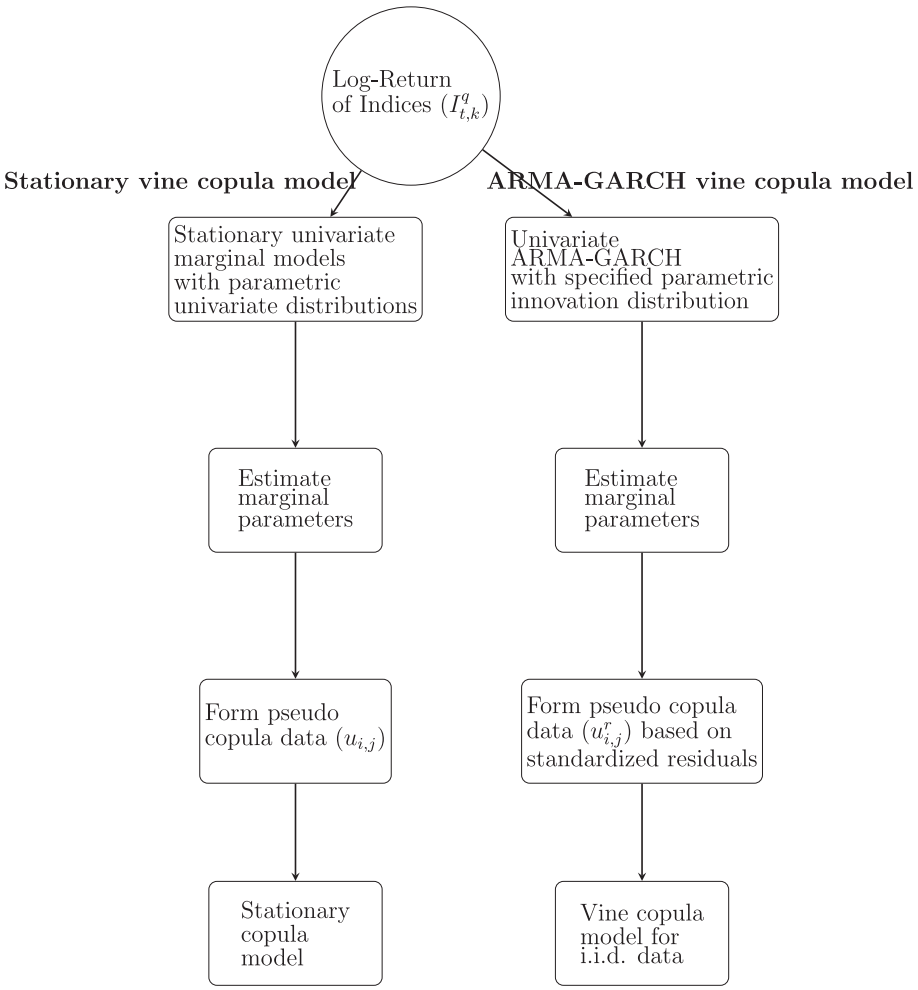

Figure A.6: Data processing differences between ARMA-GARCH and stationary vine copula models.

Appendix B. Marginal distribution and parameters from the stationary copula Modelling

Table B.8: Marginal distributions and parameters of the different indices per time period.

Period q	Time Series	Marginal Model	μ	σ	ν	ξ	loglik
2007–2009	Market Index	Skew Student-t	−0.0008	0.0364	2.1618	0.8919	2044.52
	ESG Index A	Skew Student-t	−0.0005	0.0386	2.1465	0.9194	2027.26
	ESG Index B	Skew Student-t	−0.0004	0.0256	2.5468	0.8524	1976.11
	ESG Index C	Skew Student-t	−0.0009	0.0308	2.2964	0.8738	1990.76
	ESG Index D	Skew Student-t	0.0005	0.0257	2.6695	0.9893	1911.78
2012–2012	Market Index	Skew Student-t	0.0004	0.0136	2.8494	0.9492	2348.93
	ESG Index A	Skew Student-t	0.0002	0.0124	3.2892	0.9511	2350.38
	ESG Index B	Skew Student-t	0.0005	0.0126	3.2176	0.9312	2345.92
	ESG Index C	Skew Student-t	0.0006	0.0141	3.6647	0.9501	2223.28
	ESG Index D	Skew Student-t	0.0005	0.0139	3.0558	0.9543	2295.54

(*continued*)

Period q	Time Series	Marginal Model	μ	σ	ν	ξ	loglik
2013–2015	Market Index	Skew Student-t	0.0005	0.0082	4.8037	0.9216	2600.45
	ESG Index A	Skew Student-t	0.0006	0.0086	4.6482	0.9682	2563.70
	ESG Index B	Skew Student-t	0.0005	0.0087	5.0999	0.9089	2554.87
	ESG Index C	Skew Student-t	0.0008	0.0101	5.7737	0.9432	2426.42
	ESG Index D	Skew Student-t	0.0006	0.0085	5.6388	0.9449	2555.15
2016–2019	Market Index	Skew Student-t	0.0006	0.0213	2.0820	0.9999	2659.57
	ESG Index A	Skew Student-t	0.0008	0.0136	2.3056	0.9774	2583.48
	ESG Index B	Skew Student-t	0.0007	0.0119	2.4545	0.9619	2577.86
	ESG Index C	Skew Student-t	0.0005	0.0109	2.8500	0.9252	2513.15
	ESG Index D	Skew Student-t	0.0005	0.0099	2.5922	0.9632	2655.08
2021–2022	Market Index	Skew Student-t	0.0010	0.0195	2.2623	0.9300	2367.03
	ESG Index A	Skew Student-t	0.0011	0.0186	2.3355	0.9219	2334.40
	ESG Index B	Skew Student-t	0.0013	0.0189	2.3529	0.9349	2304.94
	ESG Index C	Skew Student-t	0.0010	0.0371	2.0551	0.9466	2393.14
	ESG Index D	Skew Student-t	0.0009	0.0216	2.2209	0.9622	2336.14

Appendix C. ARMA-GARCH Vine - Tree 4

Table C.9: Static vine copula fitting results in the dependence analysis of market and ESG class indices for Tree 4 in different periods. (rot = copula family's rotation, ltaildep/utaildep = lower/upper tail dependence coefficients).

Period q	conditioned	conditioning	family	rot	tau	ltaildep	utaildep
2007–2009	D, C	B, A, M	Joe	180	0.0736	0.162	0
2010–2012	D, C	B, A, M	Joe	180	0.0481	0.109	0
2013–2015	D, C	B, A, M	t	0	0.0074	0.001	0.001
2016–2018	D, C	B, A, M	Gauss.	0	−0.1842	0	0
2019–2021	D, C	B, A, M	t	0	0.2740	0.005	0.005

Appendix D. Stationary Vine - Tree 4

Appendix D.1. Tree 4

Table D.10: Dependence across time for each period q for Tree 3. These values and families are the same for $M-3, C-2; B-2, A-2, M-2$ as the tree structure is the same. (rot = copula family's rotation, ltaildep/utaildep = lower/upper tail dependence coefficients, Gumb = Gumbel, Gauss = Gaussian, Indep = Independence).

Period q	conditioned	conditioning	family	rot	tau	ltaildep	utaildep
2007–2009	M−2, C-1	B-1, A-1, M-1	t	0	0.007	0.014	0.014
	B-2, A-1	M−1, A-2, M-2	Indep.	0	0	0	0
	A-2, B-1	A-1, M−1, M-2	Indep.	0	0	0	0
2010–2012	M−2, C-1	B-1, A-1, M-1	t	0	−0.023	0	0
	B-2, A-1	M−1, A-2, M-2	Indep.	0	0	0	0
	A-2, B-1	A-1, M−1, M-2	Indep.	0	0	0	0
2013–2015	M−2, C-1	B-1, A-1, M-1	Frank	0	−0.050	0	0
	B-2, A-1	M−1, A-2, M-2	Gauss.	0	−0.042	0	0
	A-2, B-1	A-1, M−1, M-2	Indep.	0	0	0	0
2016–2018	M−2, C-1	B-1, A-1, M-1	t	0	−0.014	0.002	0.002
	B-2, A-1	M−1, A-2, M-2	t	0	−0.033	0.007	0.007
	A-2, B-1	A-1, M−1, M-2	BB7	270	−0.032	0	0
2019–2021	M−2, C-1	B-1, A-1, M-1	Gumb.	180	0.024	0.033	0
	B-2, A-1	M−1, A-2, M-2	t	0	−0.009	0.001	0.001
	A-2, B-1	A-1, M−1, M-2	t	0	0.017	0.014	0.014

*Temporal Dependence.

Table D.11: Dependence across indices for each period q for Tree 4. These values and families are the same for $D-2, C-2; B-2, A-2, M-2$ and $D-3, C-3; B-3, A-3, M-3$ etc. as the tree structure is the same. (rot = copula family's rotation, ltaildep/utaildep = lower/upper tail dependence coefficients, Clay = Clayton).

Period q	conditioned	conditioning	family	rot	tau	ltaildep	utaildep
2007–2009	D-1, C-1	B-1, A-1, M-1	Clay.	0	0.106	0.055	0
2010–2012	D-1, C-1	B-1, A-1, M-1	BB8	180	0.059	0	0
2013–2015	D-1, C-1	B-1, A-1, M-1	t	0	0.004	0.001	0.001
2016–2018	D-1, C-1	B-1, A-1, M-1	BB1	90	−0.166	0	0
2019–2021	D-1, C-1	B-1, A-1, M-1	t	0	0.296	0.019	0.019

*Dependence across indices.

Appendix D.2. Comparison of ARMA-GARCH and stationary vine copulas

Table D.12: AICs on the original scale allowing for all copula families in all models; Different Markov Orders for S-vines, the bold entries are the best fitting model. The number of model parameters (copula and marginal) are reported in parenthesis below AIC values.

Structure Imposed	No		Yes		No	Yes
Type	Dynamic Vine Copula		Dynamic Vine Copula		Static Vine copula	
	(S-Vine)		(S-Vine)		(ARMA-GARCH vine)	
Markov	$p=1$	$p=2$	$p=1$	$p=2$	–	–
Order						
2007–2009	−27777.01	−27838.56	−27785.50	**−27849.83**	−27393.67	−27396.88
	(71)	(92)	(67)	(85)	(42)	(42)
2010–2012	−31067.84	**−31137.60**	−31059.51	−31116.09	−30919.05	−30921.14
	(58)	(69)	(61)	(72)	(43)	(43)
2013–2015	−32184.70	**−32366.08**	−32192.88	−32302.27	−32176.27	−32177.40
	(56)	(75)	(57)	(71)	(41)	(43)
2016–2018	−33027.62	−33056.91	−33051.04	−33098.55	−37269.62	**−37277.00**
	(64)	(80)	(67)	(81)	(45)	(46)
2019–2021	−32496.69	**−32626.04**	−32295.25	−32415.15	−31079.81	−31063.62
	(65)	(88)	(67)	(86)	(46)	(46)

Appendix D.3. ARMA-GARCH effects

The Autoregressive Moving Average model ($ARMA(p, q)$) is a combination of the AR order p and MA order q for the time series $\{r_t, t = 1, \ldots, T\}$ such that

$$r_t = \phi_0 + \sum_{l=1}^{p} \phi_l r_{t-l} + w_t + \sum_{k=1}^{q} \theta_k w_{t-k},$$

where $w_t \overset{i.i.d.}{\sim} \mathcal{N}(0, \sigma^2)$ denotes white noise error terms. $\theta_1, \ldots, \theta_q, \phi_1, \ldots, \phi_p$ are the parameters of the model, and ϕ_0 is the expectation of r_t.

To define the Generalized Autoregressive Conditional Heteroscedasticity (GARCH) model class, one splits the model into two components.

$$r_t = \mu_t + w_t$$

If the mean equation is parameterized the resulting model is the ARMA-GARCH model. The parameterization of the innovations $w_t = r_t - \mu_t$ called the volatility equation is following a $GARCH(m, s)$ model if it is given by

$$w_t = \sigma_t \varepsilon_t, \quad \sigma_t^2 = \alpha_0 + \sum_{i=1}^{m} \alpha_i w_{t-i}^2 + \sum_{j=1}^{s} \beta_j \sigma_{t-j}^2.$$

Thus, the innovations w_t are decomposed multiplicatively into a time dependent component σ_t and a white error term $\varepsilon_t \overset{i.i.d.}{\sim} \mathcal{N}(0, 1)$.

Skewness (ϕ) and Kurtosis (ρ) are estimated as the third and fourth central moments.

Table D.13: Different parameters of the variance, mean, distribution model for each time series and period.

	Time series	μ	ϕ	θ	ω	ϕ	ρ	α	β
2007–2009	Market Index	−0.0005	–	–	0.0004	0.8883	2.4901	0.6048	–
	ESG Index A	−0.0003	–	–	0.0004	0.9161	2.4671	0.7569	–
	ESG Index B	−0.0001	–	–	0.0000	0.8584	2.1809	–	0.9964
	ESG Index C	−0.0004	–	–	0.0004	0.8719	2.6573	0.5177	–
	ESG Index D	0.0009	–	–	0.0000	1.006	2.2100	–	0.9970
2010–2012	Market Index	0.0004	–	–	0.0000	0.9484	3.2210	–	0.9951
	ESG Index A	0.0002	–	–	0.0000	0.9498	3.3824	–	0.9902
	ESG Index B	0.0006	–	–	0.0000	0.9327	3.5234	–	0.9955
	ESG Index C	0.0005	–	–	0.0000	0.9481	3.5528	–	0.9877
	ESG Index D	0.0005	–	–	0.0000	0.9549	3.2695	–	0.9945
2013–2015	Market Index	0.0005	–	–	0.0000	0.9234178	4.4592	–	0.9902
	ESG Index A	0.0007	–	–	0.0000	0.9827	4.2107	–	0.9953
	ESG Index B	0.0005	–	–	0.0000	0.9058	4.4540	–	0.9990
	ESG Index C	0.0008	–	–	0.0000	0.9423	5.2483	–	0.9990
	ESG Index D	0.0007	–	–	0.0000	0.9426	6.2296	–	0.9975
2016–2018	Market Index	0.0006	–	−0.0589	0.0000	0.9824	2.9890	–	0.9878
	ESG Index A	0.0008	–	−0.0626	0.0000	0.9664	2.9756	–	0.9947
	ESG Index B	0.0007	–	−0.0393	0.0000	0.9497	3.1752	–	0.9916
	ESG Index C	0.0006	–	−0.0258	0.0000	0.9232	3.6257	–	0.9914
	ESG Index D	0.0005	−0.1380	0.0561	0.0000	0.9632	3.3380	–	0.9882
2019–2021	Market Index	0.0010	−0.1721	–	0.0000	0.9082	2.3145	–	0.9936
	ESG Index A	0.0011	–	–	0.0000	0.9243	2.3366	–	0.9917
	ESG Index B	0.0012	–	−0.1727	0.0000	0.9027	2.4773	–	0.9929
	ESG Index C	0.0010	–	–	0.0000	0.9451	2.2379	–	0.9911
	ESG Index D	0.0010	–	–	0.00008	0.9484	3.4061	0.7275	–

References

1. Amel-Zadeh A, Serafeim G. Why and how investors use ESG information: evidence from a global survey. *Financ Anal J*. 2018;74:87–103.
2. Revelli C. Socially responsible investing (SRI): from mainstream to margin? *Res Int Bus Finance*. 2017;39:711–717. https://doi.org/10.1016/j.ribaf.2015.11.003.
3. Global Sustainable Investment Alliance (GSIA). 2020 global sustainable investment review. In: *Technical Report. Global Sustainable Investment Alliance*; 2020. http://www.gsi-alliance.org/wp-content/uploads/2021/08/GSIR-20201.pdf. Accessed July 25, 2022.
4. Patton AJ. Modelling asymmetric exchange rate dependence. *Int Econ Rev*. 2006;47:527–556.
5. McNeil AJ, Frey R, Embrechts P. *Quantitative Risk Management: Concepts, Techniques and Tools-Revised Edition*. Princeton University Press; 2015.
6. Cherubini U, Luciano E, Vecchiato W. *Copula Methods in Finance*. John Wiley & Sons; 2004.
7. Sklar A. *Fonctions de répartition à n dimensions et leurs marges*. vol. 8. Publications de l'Institut de Statistique de L'Université de Paris; 1959:229–231.
8. Aas K, Czado C, Frigessi A, Bakken H. Pair-copula constructions of multiple dependence. *Insur Math Econ*. 2009;44:182–198.
9. Bedford T, Cooke RM. Vines–a new graphical model for dependent random variables. *Ann Stat*. 2002a;30:1031–1068.
10. Nagler T, Krüger D, Min A. Stationary vine copula models for multivariate time series. *J Econom*. 2022;227:305–324. https://doi.org/10.1016/j.jeconom.2021.11.015.
11. Bax K, Sahin Ö, Czado C, Paterlini S. *ESG, Risk, and (Tail) Dependence*. 2021. https://doi.org/10.2139/ssrn.3846739. SSRN 3846739.
12. Lööf H, Sahamkhadam M, Stephan A, et al. *Incorporating ESG into Optimal Stock Portfolios for the Global Timber & Forestry Industry*. Royal Institute of Technology, CESIS-Centre of Excellence for Science; 2022. Technical Report.
13. Górka J, Kuziak K. Volatility modeling and dependence structure of esg and conventional investments. *Risks*. 2022;10:20.
14. D'Amato V, D'Ecclesia R, Levantesi S. ESG score prediction through random forest algorithm. *Comput Manag Sci*. 2021:1–27.
15. Joe H. *Multivariate Models and Multivariate Dependence Concepts*. CRC Press; 1997b.
16. Joe H. Asymptotic efficiency of the two stage estimation method for copula-based models. *J Multivariate Anal*. 2005;94:401–419.
17. Genest C, Ghoudi K, Rivest L. A semi-parametric estimation procedure of dependence parameters in multivariate families of distributions. *Biometrika*. 1995;82:543–552.
18. Joe H. Families of m-variate distributions with given margins and m(m-1)/2 bivariate dependence parameters. In: Rüschendorf L, Schweizer B, Taylor MD, eds. *Distributions with Fixed Marginals and Related Topics*. 1996:120–141.
19. Bedford T, Cooke RM. Probability density decomposition for conditionally dependent random variables modeled by vines. *Ann Math Artif Intell*. 2001;32:245–268.

20. Hobæk Haff I, Aas K, Frigessi A. On the simplified pair-copula construction — simply useful or too simplistic? *J Multivariate Anal*. 2010;101:1296–1310.
21. Stöber J, Joe H, Czado C. Simplified pair copula constructions—limitations and extensions. *J Multivariate Anal*. 2013;119:101–118.
22. Nagler T, Czado C. Evading the curse of dimensionality in nonparametric density estimation with simplified vine copulas. *J Multivariate Anal*. 2016;151:69–89.
23. Nagler T, Schellhase C, Czado C. Nonparametric estimation of simplified vine copula models: comparison of methods. *Depend Model*. 2017;5:99–120. https://doi.org/10.1515/demo-2017-0007.
24. Czado C. *Analyzing Dependent Data with Vine Copulas: A Practical Guide with R*. Springer Nature Switzerland; 2019.
25. Hobæk Haff I, et al. Parameter estimation for pair-copula constructions. *Bernoulli*. 2013;19:462–491.
26. Stöber J, Schepsmeier U. Estimating standard errors in regular vine copula models. *Comput Stat*. 2013;28:2679–2707.
27. Akaike H. Information theory and an extension of the maximum likelihood principle. In: *Selected Papers of Hirotugu Akaike*. Springer; 1998:199–213.
28. Schwarz G. Estimating the dimension of a model. *Ann Stat*. 1978;6:461–464.
29. Morales-Nápoles O. Counting vines. In: Kurowicka D, Joe H, eds. *Dependence Modeling: Vine Copula Handbook*. World Scientific Publishing Co.; 2011:189–218.
30. Dissmann J, Brechmann EC, Czado C, Kurowicka D. Selecting and estimating regular vine copulae and application to financial returns. *Comput Stat Data Anal*. 2013;59:52–69.
31. Nagler T, Vatter T. Rvinecopulib: high performance algorithms for vine copula modeling. URL: https://vinecopulib.github.io/rvinecopulib. r package version 0.5.5.1.1; 2020.
32. Coblenz M. MATVines: a vine copula package for matlab. *SoftwareX*. 2021;14, 100700. https://doi.org/10.1016/j.softx.2021.100700. https://www.sciencedirect.com/science/article/pii/S2352711021000455.
33. Nagler T, Vatter T. *pyvinecopulib*. 2021. https://doi.org/10.5281/zenodo.5097393.
34. Refinitiv. Environmental, social and governance (ESG) scores from Refinitiv. https://www.refinitiv.com/content/dam/marketing/en_us/documents/methodology/refinitiv-esg-scores-methodology.pdf; 2021. Accessed November 4, 2022.
35. Ling S, Li WK. On fractionally integrated autoregressive moving-average time series models with conditional heteroscedasticity. *J Am Stat Assoc*. 1997;92:1184–1194.
36. Zumente I, Lāce N. Esg rating—necessity for the investor or the company? *Sustainability*. 2021;13:8940.
37. Lisin A, Kushnir A, Koryakov AG, Fomenko N, Shchukina T. Financial stability in companies with high ESG scores: evidence from north America using the ohlson o-score. *Sustainability*. 2022;14:479.
38. Beare BK, Seo J. Vine copula specifications for stationary multivariate Markov chains. *J Time Anal*. 2015;36:228–246.
39. Brechmann EC, Czado C. COPAR – multivariate time series modeling using the copula autoregressive model. *Appl Stoch Model Bus Ind*. 2015;31:495–514.
40. Smith MS. Copula modelling of dependence in multivariate time series. *Int J Forecast*. 2015;31:815–833.
41. Nagler T. Svines: stationary vine copula models. URL: https://github.com/tnagler/svines. r package version 0.1.4; 2022.
42. Cont R. Empirical properties of asset returns: stylized facts and statistical issues. *J Quant Finance*. 2001:223–236.
43. Geidosch M, Fischer M. Application of vine copulas to credit portfolio risk modeling. *J Risk Financ Manag*. 2016;9:4.
44. Pourkhanali A, Kim JM, Tafakori L, Fard FA. Measuring systemic risk using vine-copula. *Econ Modell*. 2016;53:63–74.
45. Bax K, Bonaccolto G, Paterlini S. *Do Lower ESG Rated Companies Have Higher Systemic Impact? Empirical Evidence from Europe and the United States*. 2022. https://doi.org/10.2139/ssrn.4147370. SSRN 4147370.
46. Sahin Ö, Bax K, Paterlini S, Czado C. The pitfalls of (non-definitive) Environmental, Social, and Governance scoring methodology. *Global Finance J*. 2022. https://doi.org/10.1016/j.gfj.2022.100780.
47. Berg F, Kölbel JF, Rigobon R. Aggregate confusion: the divergence of ESG ratings. *Rev Finance*. 2022. https://doi.org/10.1093/rof/rfac033.
48. Abhayawansa S, Tyagi S. Sustainable investing: the black box of environmental, social, and governance (ESG) ratings. *J Wealth Manag*. 2021;24.
49. Gyönyörová L, Stachoň M, Stašek D. ESG ratings: relevant information or misleading clue? Evidence from the S&P Global 1200. *J Sustain Finance Invest*. 2021. https://doi.org/10.1080/20430795.2021.1922062.
50. Sahin Ö, Bax K, Czado C, Paterlini S. Environmental, Social, Governance scores and the Missing pillar—why does missing information matter? *Corp Soc Responsib Environ Manag*. 2022a;29:1782–1798. https://doi.org/10.1002/csr.2326.
51. Pedersen LH, Fitzgibbons S, Pomorski L. Responsible investing: the ESG-efficient frontier. *J Financ Econ*. 2021;142:572–597.
52. Han Y, Li J. Should investors include green bonds in their portfolios? Evidence for the USA and Europe. *Int Rev Financ Anal*. 2022;80.
53. Aas K. Pair-copula constructions for financial applications: A review. *Econometrics*. 2016;4:43. https://doi.org/10.3390/econometrics4040043. https://www.mdpi.com/2225-1146/4/4/43.
54. Sommer E, Bax K, Czado C. *Vine Copula Based Portfolio Level Conditional Risk Measure Forecasting*. 2022. arXiv preprint arXiv:2208.09156.